DOI: 10.1002/chem.200600546

Anion-Binding Properties of the Tripyrrolemethane Group: A Combined Experimental and Theoretical Study

Chagit Denekamp,*[a] Kinga Suwinska,*[b] Hussein Salman,[a] Yael Abraham,[a] Yoav Eichen,*[a, c] and J. Ben Ari[a]

Abstract: Tripyrrolemethane- and bis-tripyrrolemethane-containing systems were recently reported to be efficient and selective hosts for anions. Nevertheless, the basic intrinsic properties of tripyrrolemethane as a ligand for anions have not yet been explored. Here we report the study of the anion-binding properties of the tripyrrolemethane group. We applied a combined experimental and theoretical approach to determine the affinity of the tripyrrolemethane system for different anions in the gas phase, in solution and in the crystalline state. In the crystal, the tripyrrolemethane group forms a number of different complexes with the bromide ion, some involving the participation of more than one ligand species. Despite the very similar basicity of fluoride and dihydrogen phosphate, the tripyrrolemethane ligand exhibits a clear preference for the fluoride anion in solution, which indicates an anion-binding system and not merely deprotonation. Although the affinity of the tripyrrolemethane ligand for other ions was negligible in solution, gas-phase studies show that complexation with larger halide ions is favoured over complexation with fluoride.

Keywords: anions · halides · molecular recognition · NMR titration · pyrroles

Introduction

One of the central concepts of molecular recognition is the issue of selectivity. This aspect has motivated the design of ion sensors that are based on molecular recognition processes.

Pyrrole derivatives are traditionally associated with efficient ligation to metal cations in macrocyclic systems, such as porphyrin[1] and porphyrin derivatives.[2a,1] These are very abundant in biological systems,[2] playing major roles in all sorts of biochemical transformations, such as light harvesting[3] and redox processes.[4]

In the last decade, following the pioneering work of the group headed by Sessler,[5] the anion-binding properties of pyrrole and its derivatives were studied with the aim of developing efficient and selective anion-binding ligands.[6] Calixarene analogs, termed calixpyrroles, developed over the last decade, display promising properties with respect to affinity and selectivity.[7] The rather simple synthesis of these compounds allows relatively easy derivatisation with the reporting group, thereby offering a simple and effective means of sensing the presence of ions in solution.[8] Another most promising anion ligand is the tripyrrolemethane moiety that was recently coupled to several optical-reporting groups.[1,8] Bistripyrrolemethane systems have also been proposed as promising ligands that prove to be effective and selective hosts for anions.[9] Nevertheless, the basic intrinsic properties of tripyrrolemethane as a ligand for anions have not yet been explored.

Molecular or ion recognition can be studied by NMR titration experiments, X-ray crystallography, UV-visible spectroscopy and other analytical techniques. The use of mass spectrometry to study host–guest interactions and molecular recognition involving either biological hosts or synthetic hosts has also been an enormously active area of research

[a] Dr. C. Denekamp, H. Salman, Y. Abraham, Prof. Y. Eichen, J. Ben Ari
Department of Chemistry, Technion—Israel Institute of Technology
Technion City, 32000, Haifa (Israel)
Fax: (+927) 4-8293736
E-mail: chchagit@tx.technion.ac.il
yoavoffice@gmail.com

[b] Dr. K. Suwinska
Institute of Physical Chemistry, Polish Academy of Sciences
Kasprzaka 44/52, 01 224 Warszawa (Poland)
Fax: (+48) 64-021-1478
E-mail: kinga@ichf.edu.pl

[c] Prof. Y. Eichen
Solid-State Institute, Technion—Israel Institute of Technology
Technion City, 32000, Haifa (Israel)
Fax: (+927) 4-8233735

over the past decade.[10] Electrospray ionisation (ESI) mass spectrometry allows the study of a wide variety of host–guest complexes and other noncovalent species that are formed in solution, because the process is gentle enough to allow the survival of many types of weakly bound complexes. There are a few examples of the specific use of ESI and mass spectrometry for the study of ion sensors. For example, Kubik and co-workers developed an artificial anion receptor in which two cyclohexapeptide subunits containing L-proline and 6-aminopicolinic acid subunits in an alternating sequence are connected via an adipinic acid spacer.[11] ESI mass spectrometry and NMR spectroscopic investigations showed that the bridged bis(cyclopeptide) does indeed form defined 1:1 complexes with halides, sulfate and nitrate.[11] In another study, Jurczak and co-workers presented a macrocyclic ligand containing four amide functionalities that complexes with various anions (F^-, Cl^-, AcO^-, $H_2PO_4^-$ and p-$NO_2C_6H_4O^-$).[12] NMR titration experiments, X-ray studies and ESI mass spectrometry were employed to determine the stoichiometry and selectivity. The results in solution indicated predominant formation of 1:1 complexes for all anions studied. However, the existence of a 2:1 complex was also detected.[12]

Here we report the study of the anion-binding properties of tripyrrolemethane. The interaction between tripyrrole methane and different anionic species was studied in solution, in the gas phase and in the crystalline state. Computations were applied to selected systems to improve our understanding of the experimental results.

Experimental Section

Materials: All materials, including HPLC-grade solvents, were purchased from Sigma-Aldrich and Fluka. Solvents and starting materials were used as received, unless stated otherwise. Tripyrrolemethane was prepared according to a slightly modified literature procedure.[13]

NMR spectra were recorded by using a Bruker AVANCE 500 spectrometer at 298 ± 1 K.

X-ray crystallography: Single crystals of **1a**, **1b** and **1**-Br^-, were mounted on a Nonius KappaCCD diffractometer and the data were collected with $Mo_{K\alpha}$ radiation. Intensities were collected by means of ϕ and ω scans and were processed with the Collect data collection software[14] and DENZO-SMN for cell refinement and data reduction.[15] The structures were solved by direct methods with SHELXS-97[16] and were refined with SHELXL-97[17] within the WinGX[18] package. SHELXL-97 was also used for material publication. TEXRAY was used for structure analysis and ATOMS[19] for graphics.

Mass spectrometry: All mass spectra were acquired by using an APEX III Fourier transform ion cyclotron resonance (FT-ICR) mass spectrometer (Bruker Daltonics, Billerica, MA, USA) equipped with a 4.7 T magnet (Magnex Scientific, Oxford, UK) with an Apollo electrospray ion source. Spectra were acquired in the broadband detection mode by accumulating 16–24 scans. The ESI capillary voltage was maintained at 3.3 kV, the end plate at 3 kV, the skimmer voltage was −2.5 V and the capillary exit was −10 V (all voltages indicated). Ammonium halide salts were dissolved in water (0.05 M) and further diluted in methanol to stock solutions of $5x10^{-4}$ and $5x10^{-6}$ M. A syringe pump was used to introduce solutions at a rate of 0.1–0.2 mL h^{-1}. Nitrogen was used both as nebulising and drying gas at 100°C. For the IR multiphoton dissociation (IRMPD) experiments the desired precursor ions were isolated by standard ejection pulses ("isolation shot"). IRMPD was performed by using a 25-W CO_2 IR-laser unit (Synrad, Mukilteo, WA, USA) operating at a wavelength of 10.6 μm. The diameter of the laser beam was ≈3.5 mm. The laser was aligned to the centerline of the ICR cell.

Computations: Calculations were carried out by using the GAUSSIAN 03 series of programs.[20] Geometries were optimised at the B3PW91/6-31G-(d,p) hybrid density functional level of theory and the energies of optimised structures were recalculated at the B3PW91/6-311++G(d,p) level. Structures were analysed by means of analytical frequency calculations (zero-point energies correction at the B3PW91/6-31G(d,p) level).

Results and Discussion

NMR binding studies: Tripyrrolemethane **1** was prepared in 34% yield from pyrrole and triethylorthoformate, in the presence of chloroacetic acid (Scheme 1).

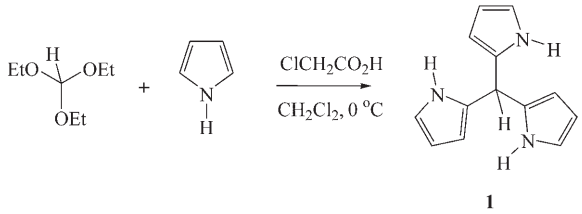

1

Scheme 1. Preparation of tripyrrolemethane, **1**.

The association of different anions to **1** was studied by means of NMR titrations. As can be seen from Figures 1 and 2, the ^1H NMR spectrum of **1** in CD_3CN and

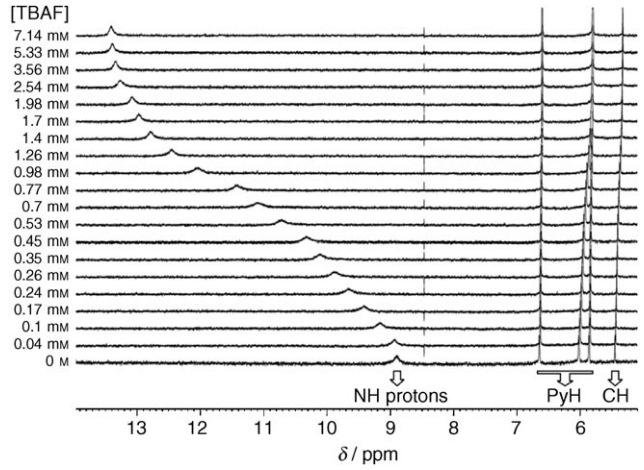

Figure 1. ^1H NMR spectra of **1** (0.5 mM) in CD_3CN in the presence of increasing concentrations of TBAF.

$[D_6]$DMSO is distinctly changed upon addition of tetrabutylammonium fluoride (TBAF). Addition of TBAF to the solutions of **1** led to downfield shifts of the pyrrole N–H peak. Upon addition of 6 mM TBAF to 0.5 mM solutions of **1** in CD_3CN, this peak shifted by ≈4.5 ppm from its initial position at $\delta = 8.9$ ppm. Similarly, under the same conditions, the

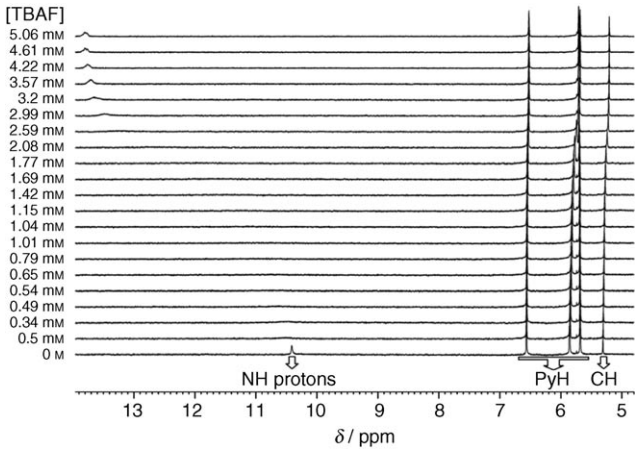

Figure 2. ^{1}H NMR spectra of **1** (0.5 mM) in [D_6]DMSO in the presence of increasing concentrations of TBAF.

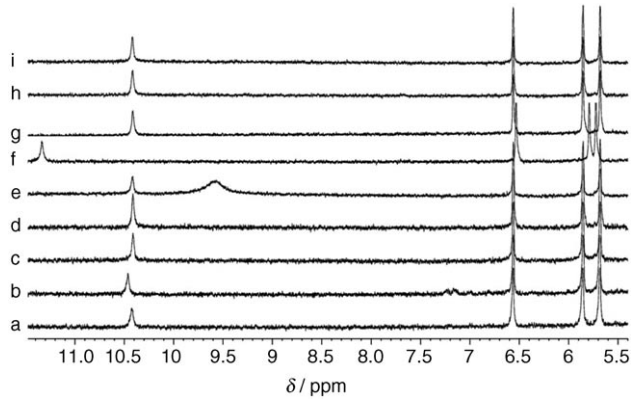

Figure 3. ^{1}H NMR titration of **1** in [D_6]DMSO before (a) and after the addition of 10 mM TBACl (b), 10 mM TBABr (c), 14 mM TBAI (d), 40 mM $TBAHSO_4$ (e), 20 mM $TBAH_2PO_4$ (f), 50 mM $TBANO_3$ (g), 50 mM $TBABF_4$ (h) and 75 mM $TBAClO_4$ (i).

N–H peak shifted by $\approx$3.4 ppm from its initial position at $\delta = 10.4$ ppm in [D_6]DMSO that contained 0.25% D_2O. In both solvents, significantly smaller guest-induced shifts ($\Delta\delta < 0.2$ ppm) were recorded for all other protons of **1**. The binding of F^- by **1** is a fast process on the NMR timescale, reaching equilibrium instantaneously at any concentration. The titration curves were successfully reproduced, assuming mixed formation of 2:1 and 1:1 host:guest complexes. The calculated binding constants are summarised in Table 1.

Table 1. Experimental binding constants for **1**-F^- and **1**-$H_2PO_4^-$ complexes.[a]

Solvent	TBAF	$TBAH_2PO_4$
[D_6]DMSO + 0.25% D_2O	$K_1 = 5000\,M^{-1}$, $K_2 = 2000\,M^{-1}$	$K_1 = 60\,M^{-1}$
[D_6]DMSO + 1% D_2O	$K_1 = 1400\,M^{-1}$, $K_2 = 1000\,M^{-1}$	$K_1 < 50\,M^{-1}$
[D_6]DMSO + 5% D_2O	$K_1 = 220\,M^{-1}$, $K_2 = 200\,M^{-1}$	$K_1 < 50\,M^{-1}$
CD_3CN	$K_1 = 41\,000\,M^{-1}$, $K_2 = 17\,000\,M^{-1}$	$K_1 = 300\,M^{-1}$

[a] In all experiments, the error was estimated to be less than $\pm$10%.

Addition of other halides and anions (as their TBA salts) led to significantly smaller guest-induced shifts, as shown in Figure 3, the only exception being $TBAH_2PO_4$. However, the association constant between **1** and $TBAH_2PO_4$ was significantly smaller than that measured for association with F^- (Table 1).

Table 1 presents the different stoichiometric ratios and association constants that were derived for fluoride and phosphate anions. NMR binding experiments show an exclusive preferential interaction between **1** and the fluoride anion. The strongest binding is revealed in pure acetonitrile, with K_1 and K_2 binding constants of 40 800 and 17 100 M^{-1}, respectively, for F^- and a K_1 of only 300 M^{-1} for a 1:1 complex with $H_2PO_4^-$.

Influence of water on the anion-binding properties of 1: Water acts as a competitive inhibitor for the formation of hydrogen-bonded complexes. In many cases, water competes with both the host and the guest.[21] Nevertheless, both the exact structure of the cavity of the host and the solvation ability of the guest play a role in the extent of water competition.[22] The effect of water on the anion-binding properties of **1** was investigated by performing ^{1}H NMR titration experiments with TBAF in [D_6]DMSO that contained increasing amounts of D_2O (Figure 4 and Table 1). The binding

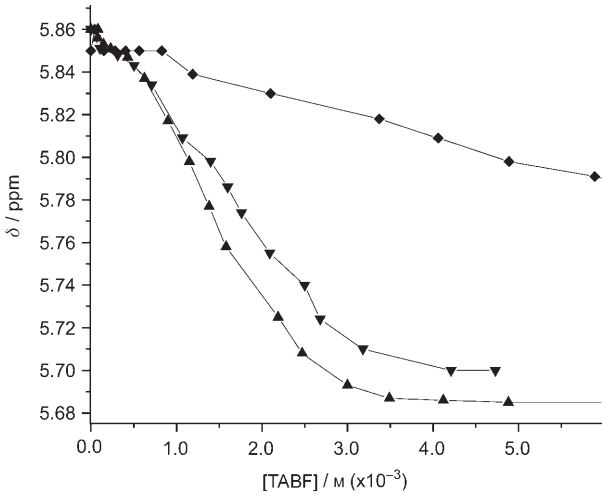

Figure 4. Titration binding curves for **1** with TBAF in [D_6]DMSO with 0.25 (▲), 1.0 (▼) and 5.0% (◆) of D_2O.

constants that were derived from these experiments clearly show a decrease in the binding efficiency between the two anions and **1** upon addition of water, indicating the importance of hydrogen bonding in the association process under investigation.

Crystal structures of 1 and its bromide complex: Crystallisation of **1** from methanol yielded two different crystalline phases that were suitable for crystallographic-structure determination.[23] The detailed structural analysis revealed that

the two phases are polymorphs of **1**, denoted as **1a** and **1b** (Figure 5). Polymorph **1a** crystallises in a noncentrosymmetric space group and consists of one *S* enantiomer, whereas polymorph **1b** crystallises in a centrosymmetric space group and consists of both *S* and *R* enantiomers. The crystal structures differ in the molecular packing, which is a consequence of their crystal symmetry.

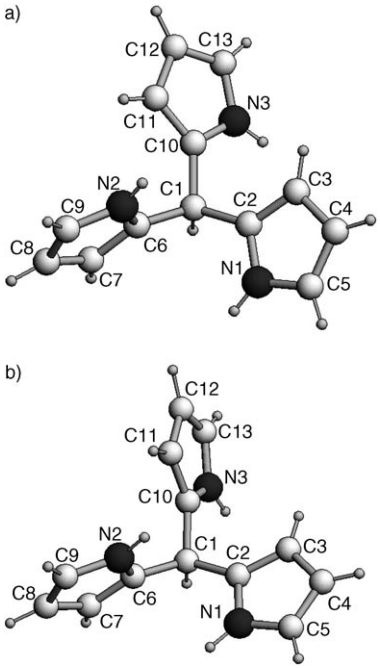

Figure 5. *S* enantiomers of **1**: a) noncentrosymmetric polymorph **1a**, b) centrosymmetric polymorph **1b**.

Crystallisation of **1** from methanol in the presence of tetrabutylammonium bromide yielded a crystalline phase that contains six crystallographically independent **1**-Br$^-$ complexes. Figure 6 shows six different **1**-Br$^-$ complexes. All complexes are dimeric in nature with a highly distorted tetrahedral coordination around the bromide ion. The complexes are interconnected and form two independent infinite chains, one consisting of complexes with **1**-Br1 and **1**-Br2 (Figure 7a), the other consisting of complexes with **1**-Br4, **1**-Br6, **1**-Br3 and **1**-Br5 (Figure 7b). The six complexes can be divided into three main families: 1) two complexes (**1**-Br1, **1**-Br2) in which one of the tripyrrolemethane groups binds the bromide ion through three N–H···Br$^-$ bonds, and a second tripyrrolemethane ligand interacts with the bromide ion through a C–H···Br$^-$ interaction; b) three

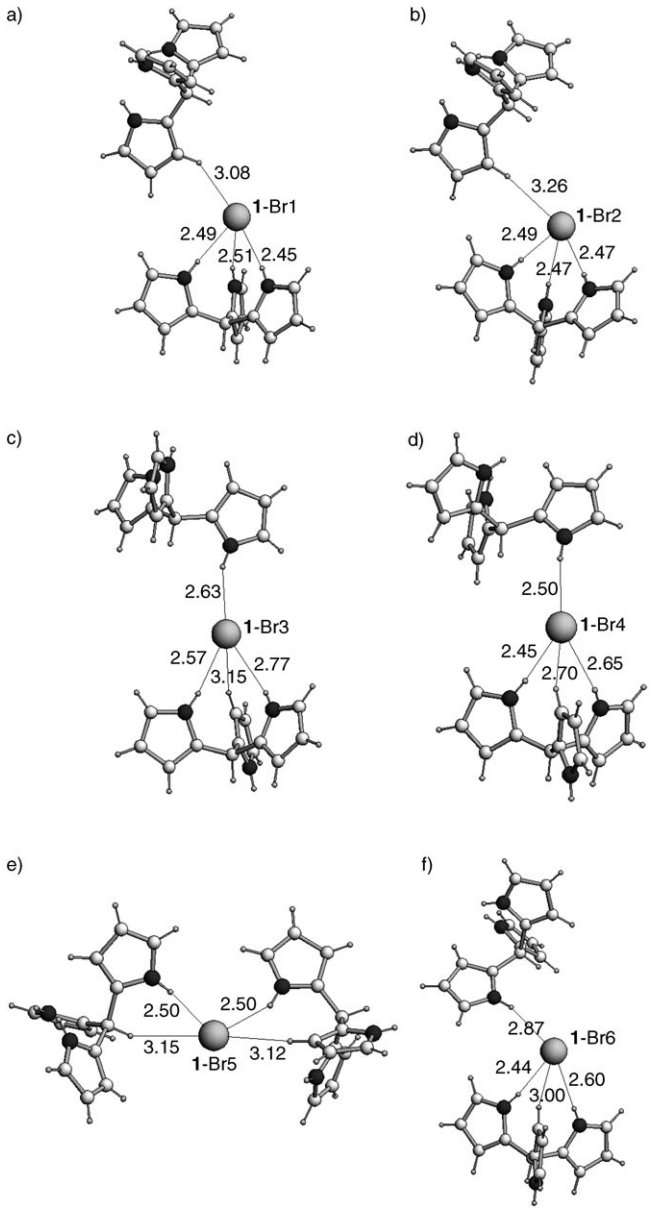

Figure 6. Six crystallographically independent complexes of **1**-Br$^-$.

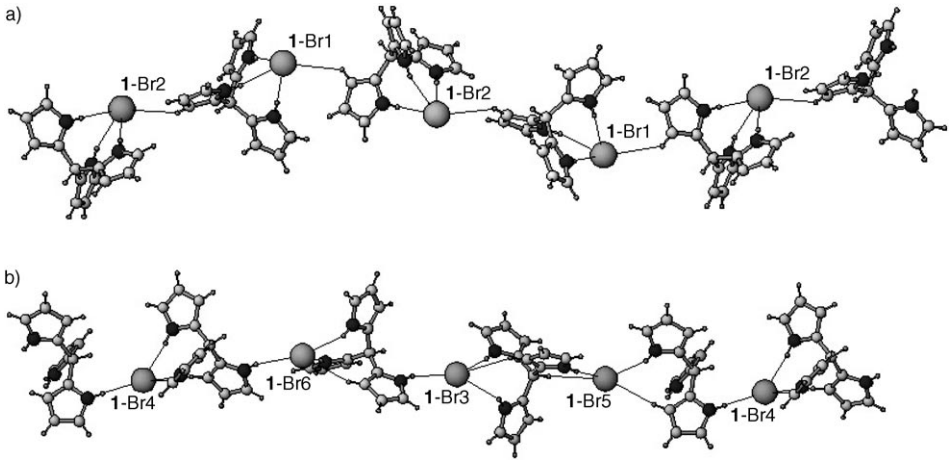

Figure 7. Two independent chains of **1**-Br$^-$ complexes found in the solid state.

complexes (**1**-Br3, **1**-Br4, **1**-Br6) in which one of the tripyrrolemethane groups binds the bromide ion through two N–H···Br$^-$ bonds and one C–H···Br$^-$ interaction, and a second tripyrrolemethane ligand contributes one N–H···Br$^-$ bond; c) one complex (**1**-Br5) in which each of the tripyrrolemethane groups binds the bromide ion through one N–H···Br$^-$ bond and one C–H···Br$^-$ interaction. Table 2 summarises the

Table 2. Hydrogen-bond lengths [Å] and angles [°] in **1**-Br$^-$.[a]

D–H···A	*d*(D–H)	*d*(H···A)	*d*(D···A)	∢(DHA)
N10–H10···Br1	0.88	2.45	3.315(7)	166.4
N11–H11···Br1	0.88	2.51	3.374(7)	169.3
N12–H12···Br1	0.88	2.49	3.368(8)	178.0
C155–H155···Br1[1]	0.95	3.08	3.763(9)	129.6
N19–H19···Br2	0.88	2.47	3.346(7)	175.6
N20–H20···Br2	0.88	2.47	3.318(7)	163.3
N21–H21···Br2	0.88	2.49	3.371(6)	177.9
C120–H120···Br2[2]	0.95	3.26	4.095(8)	147.7
N17–H17···Br3[3]	0.88	2.77	3.496(7)	141.4
N18–H18···Br3[3]	0.88	2.57	3.436(7)	170.2
N24–H24···Br3	0.88	2.63	3.450(8)	155.2
C142–H142···Br3[3]	0.95	3.15	4.027(9)	154.8
N8–H8···Br4	0.88	2.45	3.323(7)	173.1
N9–H9···Br4	0.88	2.65	3.439(8)	150.6
N14–H14···Br4[4]	0.88	2.50	3.347(7)	160.4
C103–H103···Br4	0.95	2.70	3.606(9)	160.0
N15–H15···Br5	0.88	2.50	3.307(8)	152.6
N16–H16···Br5	0.88	2.50	3.360(8)	166.9
C137–H137···Br5	0.95	3.12	4.059(9)	170.1
C138–H138···Br5	1.00	3.15	4.048(9)	150.7
N7–H7···Br6	0.88	2.87	3.717(8)	161.7
N22–H22···Br6	0.88	2.44	3.308(7)	170.3
N23–H23···Br6	0.88	2.60	3.414(7)	155.0
C176–H176···Br6	0.95	3.00	3.89(1)	157.9

[a] Symmetry transformations used to generate equivalent atoms: (1) $-x+1$, $y-\frac{1}{2}$, $-z+1$; (2) x, y, $z+1$; (3) $-x+2$, $y-\frac{1}{2}$, $-z+1$; (4) $-x+1$, $y+\frac{1}{2}$, $-z+1$.

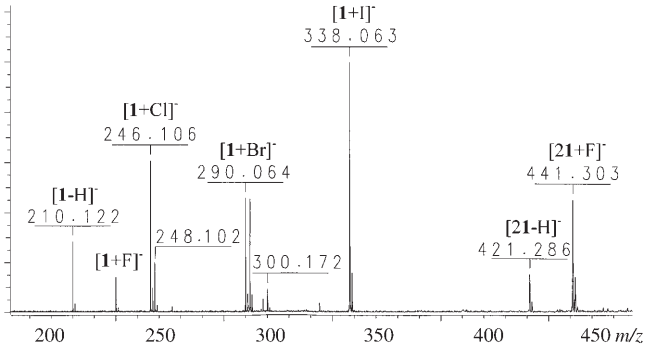

Figure 8. ESI-MS spectrum of **1** adducts with halides obtained from a solution of **1** in methanol (2×10^{-5} M) and equimolar amounts of ammonium halides (1×10^{-5} M each).

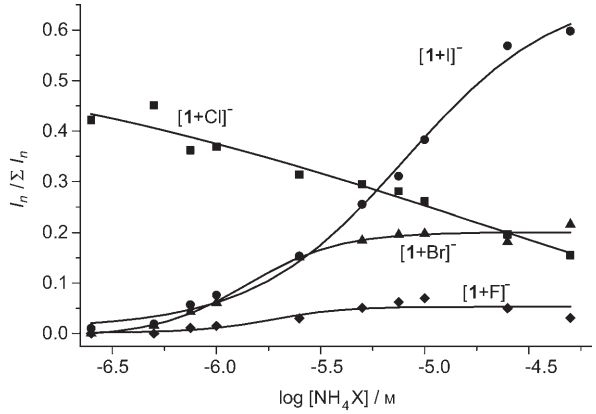

Figure 9. Formation of [**1**+X]$^-$ ions as a function of NH_4X concentration (X = F, Cl, Br, I) in an equimolar mixture of four ammonium halides in methanol. The concentration of **1** was kept constant ($\approx2\times10^{-5}$ M).

hydrogen-bond lengths and angles for the six complexes. From the complexes found in the crystal structure, it is clear that the coordination of the bromide ion is not saturated by complexation with one moiety of **1**. Figure 6 shows two independent chains of **1**-Br$^-$ complexes found in the solid state.

Mass spectrometry: Two types of mass-spectrometry experiments were performed: negative-ion attachment in solution employing ESI, and IRMPD of the resulting [**1**+X]$^-$ ions (X = F, Cl, Br and I) in the gas phase.

*Investigation of **1**-halide complexation in methanol by ESI*: Mixtures of ammonium halides and **1** in methanol were measured at different concentrations of ammonium salts. A typical ESI mass spectrum of this mixture is shown in Figure 8. All four halides give rise to [**1**+X]$^-$ ions; however, only a fluoride-bound dimer is generated under these conditions. Nevertheless, the formation of [**1**+X]$^-$ ions, for which X = I and Br, is favoured over the formation of [**1**+F]$^-$ and [2**1**+F]$^-$ together.

Figure 9 shows the complexation of **1** with the four ammonium halides as a function of the salt concentration and with a constant amount of **1**. The presence of a chloride attachment anion was observed even in pure solvents, before addition of NH_4Cl. Therefore, the relative intensity of the [**1**+Cl]$^-$ ion, *m*/*z* 246 and 248, at low concentrations is higher than other halides and drops upon addition of the salts. Clearly the generation of a [**1**+I]$^-$ ion upon addition of the halide mixture is most favoured and the formation of a [**1**+F]$^-$ ion is disfavoured, and [**1**+Cl]$^-$ and [**1**+Br]$^-$ ions are generated in moderate amounts. ESI measurements of the complexation of **1** performed separately with each ammonium halide as a function of the salt concentration also demonstrated weak complexation of **1** with the fluoride anion (Figure 10).

*IRMPD experiments on **1**-halide complexes in the gas phase*: The [**1**+X]$^-$ ions under investigation were isolated in the gas phase and were subsequently excited by an IR laser (so called IR multiphoton dissociation).[24] The irradiation time, and, thus, the internal energy, was gradually increased, inducing dissociations of the [**1**+X]$^-$ ions studied. This experiment allows evaluation of the relative barriers for bond dissociation between **1** and the halide anions. Figure 11 shows the relative survival yields of each [**1**+X]$^-$ ion as a function

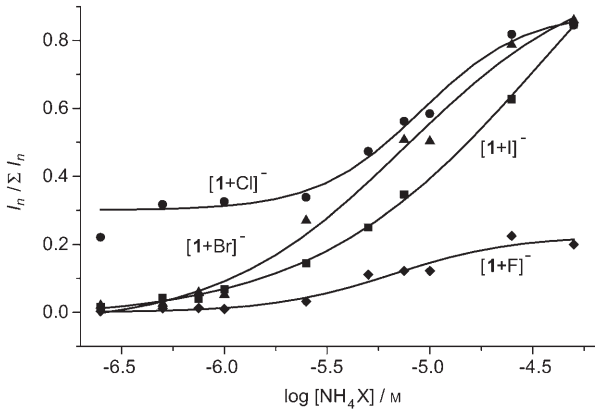

Figure 10. Formation of $[\mathbf{1}+X]^-$ ions as a function of NH_4X concentration (X = F, Cl, Br, I) measured separately for each ammonium halide in methanol. The concentration of **1** was kept constant ($\approx 2\times10^{-5}$ M).

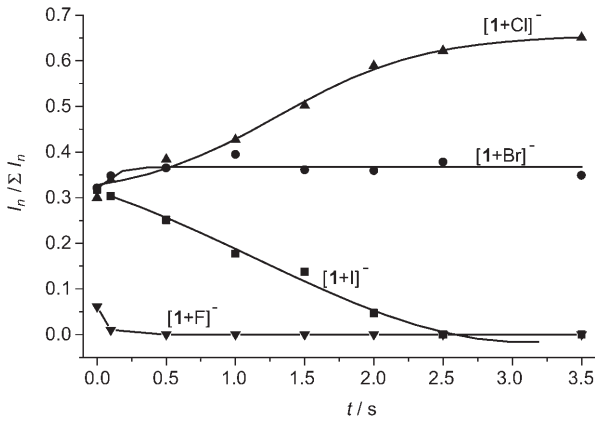

Figure 11. Relative abundance of $[\mathbf{1}-X]^-$ ions as irradiation time increases. The laser power applied was 20% of the maximum available.

of irradiation time. Assuming that dissociation barriers correlate to bond strength, it is clear that the gas-phase **1**–X bond strengths are in the order Cl > Br > I ≫ F.

However, the dissociation of $[\mathbf{1}+F]^-$ and $[\mathbf{1}+Cl]^-$ ions results in the loss of HX ($[\mathbf{1}-H]^-$ product ion), whereas $[\mathbf{1}+Br]^-$ and $[\mathbf{1}+I]^-$ ions dissociate into neutral **1** and X^- ions, exclusively (Scheme 2).

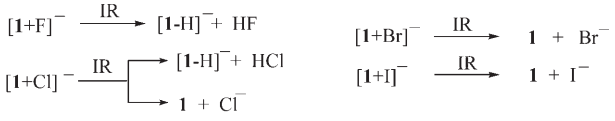

Scheme 2. Fragmentation products for $[\mathbf{1}+X]^-$ ions (X = F, Cl, Br and I), HX elimination versus detachment of X^-.

The deuterium-isotope effect in the dissociation of $[\mathbf{1}-X]^-$ anions was also investigated. The $[\mathbf{1}(D_3)+X]^-$/$[\mathbf{1}(H_3)+X]^-$ ion ratios were monitored as a function of the irradiation time. Figure 12 shows that the amount of $[\mathbf{1}(D_3)+X]^-$ is either reduced (X = Br, I) or remains constant (X = Cl) upon activation, indicating an inverse isotope effect

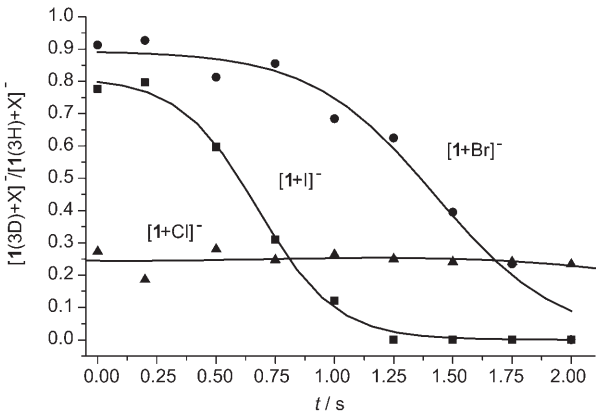

Figure 12. $[\mathbf{1}(D_3)+X]^-/[\mathbf{1}(H_3)+X]^-$ ion ratios as a function of irradiation time to deduce the direction of the H/D isotope effect. The laser power applied was 10% of the maximum available.

in the case of bromide and iodide complexes and no isotope effect in the case of the chloride. As mentioned above, $[\mathbf{1}+Cl]^-$ ions lose both the HCl and neutral **1**, whereas $[\mathbf{1}+Br]^-$ and $[\mathbf{1}+I]^-$ ions give rise to X^- ions, exclusively. The formation of neutral **1** that retains the N–H(D) bond should be faster in $\mathbf{1}(D_3)$ because an N–H(D) bond is strengthened during dissociation.

DFT calculations: Complexation of **1** with fluoride and chloride anions was studied by means of density functional theory (DFT) calculations. Complexation of halide anions by a calix[4]pyrrole was studied previously by Pichierri[25] who showed that the complexation energy depends on the electronegativity of the halide anion, namely, in the order $F^- > Cl^- > Br^- > I^-$.

The optimised structure of **1** and its fluoride and chloride adducts (B3PW91/6-31G(d,p))[26] are depicted in Figure 13. Free **1** retains a C_{3h} symmetry; however, upon complexation, it undergoes a significant conformational change to attach the halide anion by three equivalent N–H···X^- hydrogen

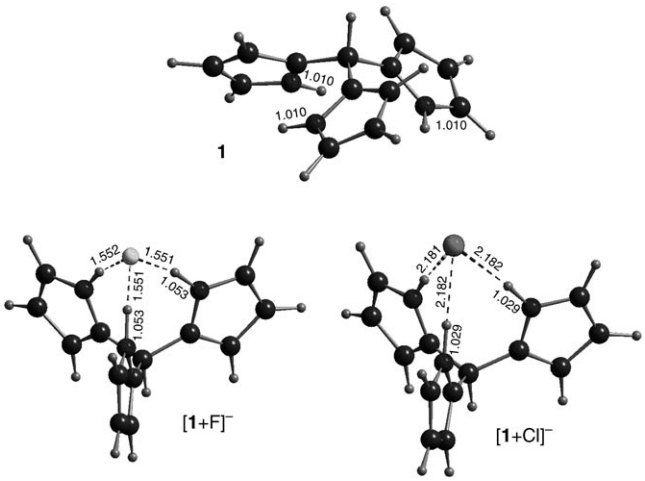

Figure 13. Calculated geometries of $[\mathbf{1}+F]^-$, $[\mathbf{1}+Cl]^-$ and free **1** optimised at B3PW91/6-31G(d,p).

bonds, resulting in a C_{3v} point-group structure. The most noticeable change in the structural parameters was observed for the N–H distances. Thus, the average N–H bond length is 1.01 Å, 1.03 Å and 1.05 Å in free **1**, [**1**+Cl]$^-$ and [**1**+F]$^-$, respectively. The F···H distance in the [**1**+F]$^-$ complex is significantly shorter than the Cl···H distance in the [**1**+Cl]$^-$ ion, namely, 1.55 Å and 2.18 Å, respectively.

As mentioned above, only a fluoride-bound dimer ([2**1**+F]$^-$) was observed in the ESI mass spectrum of **1** in the halide salt mixture, whereas other halides afforded monomers. For comparison, the geometries of two dimers [2**1**+F]$^-$ and [2**1**+Cl]$^-$ were optimised and the results are shown in Figure 14. The calculated structures show that the

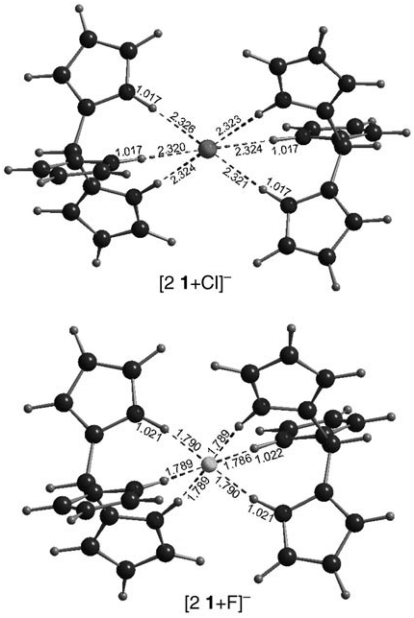

Figure 14. Geometries of chloride [2**1**+Cl]$^-$ and fluoride [2**1**+F]$^-$ halide-bound dimers optimised at B3PW91/6-31G(d,p).

X···H distances in the [2**1**+Cl]$^-$ and [2**1**+F]$^-$ dimers are greater than those in the [**1**+Cl]$^-$ and [**1**+F]$^-$ monomers by 0.14 and 0.24 Å, respectively. This indicates less stabilisation in the formation of a fluoride-bound dimer than for its chloride analog. Surprisingly, however, the relative dimerisation energies indicate otherwise (Table 3).

Binding energy: The binding energy of fluoride and chloride anions to **1** is of great interest because gas-phase IRMPD measurements and theoretical calculations may be qualitatively compared. The computed binding energies of [**1**+F]$^-$, [**1**+Cl]$^-$ and their corresponding dimeric ions are reported in Table 3 and were calculated according to Equation (1):

$$\Delta E = E([n\mathbf{1}-\mathrm{X}]^-) - E(n\mathbf{1}) - E(\mathrm{X}^-) \qquad (1)$$

in which $n=1,2$ (energies with zero-point correction, ZPE). A comparison of the anion-binding energies of fluoride and chloride to **1** shows that complexation with fluoride is more

Table 3. Calculated total energies, zero-point vibrational energies and binding energies of [**1**+X]$^-$ (X = F and Cl) anion monomer and dimer complexes.

	Total energy[a] [a.u.]	ZPE[b] [kcal mol^{-1}]	Binding energy [kcal mol^{-1}]
1	−667.35863	150.2	–
[**1**−H$^+$]$^-$	−666.80359	140.9	–
[**1**+F]$^-$	−767.30833	150.6	−64.6
[2**1**+F]$^-$	−1434.70722	303.0	−87.4
[**1**+Cl]$^-$	−1127.66160	150.2	−36.3
[2**1**+Cl]$^-$	−1795.04777	300.8	−52.8

[a] Calculated at the B3PW91/6-311++G(d,p)//B3PW91/6-31G(d,p) level of theory. [b] ZPV energies were calculated at the B3PW91/6-31G-(d,p) level.

exothermic than with chloride (−64.6 and −36.3 kcal mol^{-1}, respectively). On the other hand, calculated reaction energies for the loss of HX from [**1**+X]$^-$ indicate that the elimination of HF is more favourable than the elimination of HCl [Eq. (2) and (3)]:

$$[\mathbf{1}+\mathrm{F}]^- \rightarrow [\mathbf{1}-\mathrm{H}]^- + \mathrm{HF} \qquad \Delta E = 33.8\ \mathrm{kcal\,mol^{-1}} \qquad (2)$$

$$[\mathbf{1}+\mathrm{Cl}]^- \rightarrow [\mathbf{1}-\mathrm{H}]^- + \mathrm{HCl} \qquad \Delta E = 44.5\ \mathrm{kcal\,mol^{-1}} \qquad (3)$$

The two possible dissociation products, Cl$^-$ and [**1**−H]$^-$, were observed in the ICR IRMPD studies of the [**1**+Cl]$^-$ complex. The energy difference for these two pathways was computed to be 8.2 kcal mol^{-1}, in favour of the formation of a Cl$^-$ anion. Apparently, the gap of 8.2 kcal mol^{-1} is small enough for both dissociation products to be observed under the current experimental conditions. For the [**1**+F]$^-$ complex, the computed difference for the two decomposition pathways was 30.8 kcal mol^{-1} in favour of HF loss and indeed, the only product observed in the IRMPD of [**1**+F]$^-$ was the [**1**−H]$^-$ anion. These findings indicate that, despite the stronger fluoride binding in the [**1**+F]$^-$ complex (relative to Cl$^-$), it loses HF easily. This trend may be extended reasonably to bromide and iodide complexes with **1** in which only X$^-$ ions were observed as the IRMPD products, indicating weaker binding of these halides to **1**.

Conclusion

NMR titration experiments show an explicit tendency of **1** to complex fluoride ions, and a much lower tendency for phosphate anions. This interaction is based on hydrogen bonding, as shown by competition experiments of water binding. Furthermore, fluoride complexes are dimeric and the formation of higher aggregates cannot be ruled out. Support for the possible formation of intermolecular arrays was obtained from the crystal structure of the bromide-bound complex. ESI experiments with the four halide salts did not reveal a strong and selective interaction of **1** with fluoride. Conversely, they did indicate that formation of [**1**+X]$^-$ ions, for which X = I and X = Br, in methanol is favoured over the formation of [**1**+F]$^-$ and [2**1**+F]$^-$ together. IRMPD ex-

periments showed that $[\mathbf{1}+X]^-$ ions give rise to X^- and neutral **1** (if X = Br, I), and both Cl^- (with neutral **1**) and $[\mathbf{1}-H]^-$ ions (with HCl) (if X = Cl), and if X = F, the dissociation products are $[\mathbf{1}-H]^-$ and HF. The order of stabilisation of $[\mathbf{1}+X]^-$ ions in the gas phase was Cl > Br > I > F, and there was a reversed deuterium-isotope effect for the dissociation of $\mathbf{1}(D_3)$ (X = Br, I), as expected for N–H bond strengthening. A comparison of the relative gas-phase stability of $[\mathbf{1}+X]^-$ ions (Cl > Br > I > F) with that observed under electrospray conditions (I > Br ≈ Cl > F) in methanol indicates the strong solvent effect on the complexation phenomenon studied. The only anion that generated a dimer rather than a monomer is fluoride, which also showed a different behaviour upon IR activation. There is, therefore, strong evidence that the complexation of Cl^-, Br^- and I^- is fundamentally different from complexation with F^-. This is in agreement with NMR investigations that indicate a particular complexation behaviour of both F^- and $H_2PO_4^-$ with **1**. In other words, both fluoride and phosphate anions behave as bases and form aggregates in solution. Additional support for the basic nature of the fluoride complex, which tends do undergo low-energy HF elimination, was obtained by appropriate DFT calculations. The dissociation experiments in the gas phase were carried out to evaluate relative association tendencies in a solventless environment that correlates with computations. However, because a competing dissociation process occurs in the case of $[\mathbf{1}+F]^-$, it is the gas-phase association process that we should examine. This was not conducted due to experimental limitations.

[1] a) J. E. Falk, *Porphyrins and Metalloporphyrins*, Elsevier, Amsterdam, **1964**; b) J. W. Buchler, *J. Porphyrins Phthalocyanines* **2000**, *4*, 337–339.

[2] a) A. J. Hoff, J. Deisenhofer, *Phys. Rep.* **1997**, 287, 1–247; b) B. Ward, A. Skorobogaty, J. C. Dabrowiak, *Biochemistry* **1986**, *25*, 6875–6883; c) B. Meunier, *Chem. Rev.* **1992**, *92*, 1411–1456; d) I. Stojiljkovic, K. Hantke, *Mol. Microbiol.* **1994**, *13*, 719–732.

[3] a) J. Deisenhofer, O. Epp, K. Miki, R. Huber, H. Michel, *Nature* **1985**, *318*, 618–624; b) G. Feher, J. P. Allen, M. Y. Okamura, D. C. Rees, *Nature* **1989**, *339*, 111–116; c) G. McDermott, S. M. Prince, A. A. Freer, A. M. Hawthornthwaite-Lawless, M. Z. Papiz, R. J. Cogdell, N. W. Isaacs, *Nature* **1995**, *374*, 517–521; d) S. M. Prince, M. Z. Papiz, A. A. Freer, G. McDemott, A. M. Hawthornthwaite-Lawless, R. J. Codgell, N. W. Isaacs, *J. Mol. Biol.* **1997**, *268*, 412–423; e) J. M. Olson, *Photochem. Photobiol.* **1998**, *67*, 61–75.

[4] a) M. Polonovski, M. F. Jayle, G. Fraudet, *Compt. Rend.* **1941**, *213*, 887–889; b) P. George, D. H. Irvine, *Nature* **1951**, *168*, 164–165; c) J. F. Gibson, D. J. E. Ingram, P. Nicholls, *Nature* **1958**, *181*, 1398–1399; d) J. F. Gibson, D. J. E. Ingram, *Nature* **1956**, *178*, 871–872; e) T. Yonetani, H. Schleyer, *J. Biol. Chem.* **1967**, *242*, 1974–1979.

[5] J. L. Sessler, M. J. Cyr, V. Lynch, E. McGhee, J. A. Ibers, *J. Am. Chem. Soc.* **1990**, *112*, 2810–2813.

[6] a) J. L. Sessler, S. Camiolo, P. A. Gale, *Coord. Chem. Rev.* **2003**, *240*, 17–55; b) J. L. Sessler, L. R. Eller, W.-S. Cho, S. Nicolaou, A. Aguilar, J. T. Lee, V. M. Lynch, D. J. Magda, *Angew. Chem.* **2005**, *117*, 6143–6146; *Angew. Chem. Int. Ed.* **2005**, *44*, 5989–5992; c) I. E. D. Vega, P. A. Gale, M. E. Light, S. J. Loeb, *Chem. Commun.* **2005**, 4913–4915; d) H. Miyaji, H.-K. Kim, E.-K. Sim, C.-K. Lee, W.-S. Cho, J. L. Sessler, C.-H. Lee, *J. Am. Chem. Soc.* **2005**, *127*, 12510–12512; e) R. Li, L. S. Evans, D. S. Larsen, P. A. Gale, S. Brooker, *New J. Chem.* **2004**, *28*, 1340–1343; f) S. V. Shevchuk, V. M. Lynch, J. L. Sessler, *Tetrahedron* **2004**, *60*, 11283–11291.

[7] a) R. Nishiyabu, P. Anzenbacher, Jr., *J. Am. Chem. Soc.* **2005**, *127*, 8270–8271; b) P. A. Gale, P. Anzenbacher, Jr., J. L. Sessler, *Coord. Chem. Rev.* **2001**, *222*, 57–102.

[8] O. D. Fox, T. D. Rolls, P. D. Beer, M. G. B. Drew, *Chem. Commun.* **2001**, 1632–1633.

[9] C. B. Reese, H. Yan, *Tetrahedron Lett.* **2001**, *42*, 5545–5547.

[10] a) J. S. Brodbelt, *Int. J. Mass Spectrom.* **2000**, *200*, 57–69; b) M. Vincenti, *J. Mass Spectrom.* **1995**, *30*, 925–939; c) M. Przybylski, M. O. Glocker, *Angew. Chem.* **1996**, *108*, 878–899; *Angew. Chem. Int. Ed. Engl.* **1996**, *35*, 806–826; d) B. N. Pramanik, P. L. Bartner, U. A. Mirza, Y.-H. Liu, A. K. Ganguly, *J. Mass Spectrom* **1998**, *33*, 911–920; e) C. A. Schalley, *Int. J. Mass Spectrom.* **2000**, *194*, 11–39.

[11] S. Kubik, R. Kirchner, D. Nolting, J. Seidel, *J. Am. Chem. Soc.* **2002**, *124*, 12752–12760.

[12] A. Szumna, J. Jurczak, *Eur. J. Org. Chem.* **2001**, 4031–4039.

[13] C. B. Reese, H. Yan, *Tetrahedron Lett.* **2001**, *42*, 5545–5547.

[14] "Collect" data collection software, B. V. Nonius, **1998**.

[15] Z. Otwinowski, W. Minor in *Processing of X-ray Diffraction Data Collected in Oscillation Mode, Methods in Enzymology,: Macromolecular Crystallography, Part A, Vol. 276* (Eds.: C. W. Carter, Jr., R. M. Sweet), Academic Press, **1997**, p. 307–326.

[16] G. M. Sheldrick, *Acta Crystallogr. Sect. A* **1990**, *46*, 467–473.

[17] G. M. Sheldrick, SHELXL-97, Program for the Refinement of Crystal Structures **1997**, University of Göttingen, Göttingen (Germany).

[18] L. J. Farrugia, *J. Appl. Crystallogr.* **1999**, *32*, 837–838.

[19] E. Dowty, ATOMS. A Computer Program for Displaying Atomic Structures **2004**, SHAPE SOFTWARE, Kingsport, USA.

[20] Gaussian 03, Revision C.02, M. J. Frisch, G. W. Trucks, H. B. Schlegel, G. E. Scuseria, M. A. Robb, J. R. Cheeseman, J. A. Montgomery, Jr., T. Vreven, K. N. Kudin, J. C. Burant, J. M. Millam, S. S. Iyengar, J. Tomasi, V. Barone, B. Mennucci, M. Cossi, G. Scalmani, N. Rega, G. A. Petersson, H. Nakatsuji, M. Hada, M. Ehara, K. Toyota, R. Fukuda, J. Hasegawa, M. Ishida, T. Nakajima, Y. Honda, O. Kitao, H. Nakai, M. Klene, X. Li, J. E. Knox, H. P. Hratchian, J. B. Cross, V. Bakken, C. Adamo, J. Jaramillo, R. Gomperts, R. E. Stratmann, O. Yazyev, A. J. Austin, R. Cammi, C. Pomelli, J. W. Ochterski, P. Y. Ayala, K. Morokuma, G. A. Voth, P. Salvador, J. J. Dannenberg, V. G. Zakrzewski, S. Dapprich, A. D. Daniels, M. C. Strain, O. Farkas, D. K. Malick, A. D. Rabuck, K. Raghavachari, J. B. Foresman, J. V. Ortiz, Q. Cui, A. G. Baboul, S. Clifford, J. Cioslowski, B. B. Stefanov, G. Liu, A. Liashenko, P. Piskorz, I. Komaromi, R. L. Martin, D. J. Fox, T. Keith, M. A. Al-Laham, C. Y. Peng, A. Nanayakkara, M. Challacombe, P. M. W. Gill, B. Johnson, W. Chen, M. W. Wong, C. Gonzalez, J. A. Pople, Gaussian, Inc, Wallingford CT, **2004**.

[21] a) L. Pauling, D. Pressman, *J. Am. Chem. Soc.* **1945**, *67*, 1003–1012; b) G. A. Jeffrey, *An Introduction to Hydrogen Bonding*, Oxford University Press, New York, **1997**; c) J. Israelachvili, *Intermolecular and Surface Forces*, 2nd ed., Academic Press: London, **1992**.

[22] a) W. W. H. Wong, M. S. Vickers, A. R. Cowley, R. L. Paul, P. D. Beer, *Org. Biomol. Chem.* **2005**, *3*, 4201–4208; b) C. Schmuck, M. Schwegmann, *Org. Lett.* **2005**, *7*, 3517–3520; c) C. Schmuck, U. Machon, *Chem. Eur. J.* **2005**, *11*, 1109–1118; d) E. Klein, M. P. Crump, A. P. Davis, *Angew. Chem.* **2004**, *117*, 302–306; *Angew. Chem. Int. Ed.* **2005**, *44*, 298–302; e) R. D. Hubbard, S. R. Horner, B. L. Miller, *J. Am. Chem. Soc.* **2001**, *123*, 5810–5811; f) V. Kral, O. Rusin, F. P. Schmidtchen, *Org. Lett.* **2001**, *3*, 873–876; g) N. Sugimoto, D. Miyoshi, J. Zou, *Chem. Commun.* **2000**, 2295–2296; h) S. Anderson, U. Neidlein, V. Gramlich, F. Diederich, *Angew. Chem.* **1995**, *107*, 1722–1726; *Angew. Chem. Int. Ed. Engl.* **1995**, *34*, 1596–1600; i) Y. Aoyama, Y. Tanaka, H. Toi, H. Ogoshi, *J. Am. Chem. Soc.* **1988**, *110*, 634–635.

[23] Crystallographic data for **1a**: $C_{13}H_{13}N_3$, $M_r = 211.26$, colourless block, $0.40 \times 0.15 \times 0.05\ mm^3$, orthorhombic, space group $P2_12_12_1$ (no. 19), $a = 5.6280(3)$ $b = 10.6490(8)$ $c = 17.850(4)$ Å, $V = 1069.8(1)$ Å^3, $Z = 4$, $\rho_{cald} = 1.312\ g\,cm^{-3}$, $F_{000} = 448$, $Mo_{K\alpha}$ radiation, $\lambda = 0.71073$ Å, $T = 150(2)$ K, $2\theta_{max} = 49.5°$, 7425 reflections collected, 1827 unique ($R_{int} = 0.089$). Final GooF = 1.16, $R = 0.064$, $wR = 0.106$, R indices based on 1544 reflections with $I > 2\sigma(I)$ (refinement on

F^2), 198 parameters. Lorentzian polarisation and absorption corrections applied, $\mu = 0.081\ mm^{-1}$. All H atoms were located in electron-density maps and were refined isotropically. Crystal data for **1b**: $C_{13}H_{13}N_3$, $M_r = 211.26$, colourless block, $0.35 \times 0.20 \times 0.06\ mm^3$, monoclinic, space group $P2_1/c$ (no. 14), $a = 5.5865(3)$ $b = 16.926(1)$ $c = 12.1102(9)$ Å, $\beta = 108.404(4)°$, $V = 1086.6(1)$ Å^3, $Z = 4$, $\rho_{cald} = 1.291\ g\,cm^{-3}$, $F_{000} = 448$, $\lambda = 0.71073$ Å, $T = 150(2)$ K, $2\theta_{max} = 46.5°$, 5705 reflections collected, 1540 unique ($R_{int} = 0.047$). Final GooF = 1.11, $R = 0.057$, $wR = 0.097$, R indices based on 1170 reflections with $I > 2\sigma(I)$ (refinement on F^2), 198 parameters. Lorentzian polarisation and absorption corrections applied, $\mu = 0.080\ mm^{-1}$. All H atoms were located in electron-density maps and were refined isotropically. Crystal data for **1**-Br$^-$: $C_{13}H_{13}N_3 \cdot C_{16}H_{36}N \cdot Br$, $M_r = 533.63$, brown block, $0.20 \times 0.15 \times 0.15\ mm^3$, monoclinic, space group $P2_1$ (no. 4), $a = 9.5322(1)$ $b = 33.1615(5)$ $c = 28.8629(5)$ Å, $\beta = 98.965(1)°$, $V = 9012(1)$ Å^3, $Z = 14$, $\rho_{cald} = 1.180\ g\,cm^{-3}$, $F_{000} = 3432$, $Mo_{K\alpha}$ radiation, $\lambda = 0.71073$ Å, $T = 100(2)$ K, $2\theta_{max} = 49.4°$, 78823 reflections collected, 29659 unique ($R_{int} = 0.100$). Final GooF = 1.05, $R = 0.093$, $wR = 0.150$, R indices based on 21433 reflections with $I > 2\sigma(I)$ (refinement on F^2), 1868 parameters, 1 restraint. Lorentzian polarisation and absorption corrections applied, $\alpha = 1.390\ mm^{-1}$. H atoms were included in geometric positions and were refined as "riding" atoms with isotropic thermal parameters based upon the corresponding bonding carbon atom [$U_{iso} = 1.2\,U_{eq}$ ($U_{iso} = 1.5\,U_{eq}$ for CH_3)].

[24] See, for example: a) D. S. Bomse, R. L. Woodin, J. L. Beuchamp, *J. Am. Chem. Soc.* **1979**, *101*, 5503–5512; b) D. S. Bomse, J. L. Beuchamp, *J. Am. Chem. Soc.* **1981**, *103*, 3292–3296; c) R. L. Woodin, D. S. Bomse, J. L. Beuchamp, *J. Am. Chem. Soc.* **1978**, *100*, 3248–3250.

[25] F. Pichierri, *J. Mol. Struct: THEOCHEM* **2002**, 581, 117–127.

[26] Different computational methods were tested and compared on a pyrrole-halide model system to establish the best functional and basis sets to be used.

Received: April 17, 2006
Published online: September 25, 2006

